UST
Morgan

FINAL REPORT

for

ULTRAVIOLET IMAGE CONVERTER TUBE DEVELOPMENT

(20 December 1964 - 20 August 1965)

Contract No.: NAS5-9111

Prepared by

Electro-Mechanical Research, Inc.
Princeton, New Jersey

for

National Aeronautics & Space Administration
Goddard Space Flight Center
Greenbelt, Maryland

R. E. Friebertshauser
Project Engineer

Martin Rome
Director, Research & Development

SUMMARY

The development of a magnetically focused, uv sensitive, image converter tube is described. Included is a description of envelope design, cathode characteristics, test results and packaging details.

The basic design goals of high resolution, linearity and "solar blindness" have been met by the proposed design. The radiant gain was lower than anticipated due to the use of the high resolution phosphor.

The 10^4 difference in response between 1216 Å and 3000 Å was achieved with a CsI photocathode; some improvement in solar blindness could be obtained by using KBr cathodes at some sacrifice in peak Q.E. at 1216 Å. The use of a fiber optic output window would make possible more versatile optical coupling to other readout devices.

TABLE OF CONTENTS

LIST OF ILLUSTRATIONS

INTRODUCTION

The development of an Image Converter Phototube for the Far Ultraviolet is described. This tube has high resolution capability and to meet this requirement uses magnetic focusing. A solar blind photocathode of CsI is employed to achieve 10^4 attenuation of 3000 Å response contrasted with the high uv quantum efficiency at 1216 Å. Compactness of packaging was achieved without adversely degrading the linearity of the output image.

1. TUBE DESIGN

1.1 Envelope Design

The specifications of resolution at 50 lp/mm minimum and plano-parallel surface window configuration determined the need for a magnetic focus tube design. In addition, at the operating voltage of 20-30 kv required for adequate gain, some method of achieving a uniform potential distribution along the axis of the tube was dictated to provide linearity and prevent envelope wall charging. The obvious means of achieving this latter requirement was the use of the parallel kovar-glass ring design outlined in the original proposal. The mechanical fabrication techniques have been perfected for the EMR photomultiplier tubes and the design make possible a very rugged, mechanically reliable tube. The image converter tube design as initially conceived was based on a 1 kv potential gradient per ring which would require 19 rings for 20 kv operation. Since it was assumed that dividing resistors would be required to establish the proper voltage gradient along the rings, 80-500 volt resistors would be needed to divide 20 kv with a 100% safety factor. On the basis of resistor reliability, this design concept appeared undesirable and an alternative method was sought to achieve the proper voltage distribution. It was on this basis that some effort was devoted to achieve an internal voltage distribution by means of evaporated metallic rings bridged by an evaporated resistive array. This effort was in parallel with the kovar-glass ring design effort. Some success was achieved with the internal resistor design but at the time this technique was developed it was determined that resistors were not required for voltage division along the kovar rings and no further effort was devoted to the evaporated technique. The voltage division is accomplished by the inherent resistivity of the 7052 glass spacer rings.

Once the basic design concept was established it was only necessary to establish a length which would provide proper voltage insulation between rings and permit operation at 20-30 kv. Experimental tubes were constructed to evaluate 5, 7 and 9 ring structures; with data obtained on these tubes the final design was established at 7 rings and an overall length of 3.66 inches. A cross-section of the envelope is illustrated in Figure 1.

1.2 Window Support and Seal

The LiF window sealing technique using silver chloride, as used on the uv photomultiplier tube, was used without modification. No trouble was experienced in this area. An additional ring was added to the photocathode window support to achieve a uniformly flat potential field beyond the active cathode diameter to minimize non-linear distortion at the cathode surface. Electrostatic field plots verified the expected advantages to be gained by the addition of this field flattening ring. The improvement can also be observed in comparison of tubes made with and without the ring.

1.3 Lithium Fluoride Window

The first tubes assembled used cleaved LiF windows since ultimate resolution was not needed in the early development phase.

As the development progressed, increased attention was devoted to the window configuration and transmission. The cleaved windows had transmissions of 50-52%. The first polished windows varied in transmission between 40 and 44% at 1216 Å, and there was some suspicion that the polishing operation was in some manner causing reduced transmission. The next crystals used were polished on one side only and the transmission of these crystals varied between 51 and 54% at 1216 Å. Recently three cleaved crystals were initially measured at 64-68%, returned for polishing of one side and subsequent transmission measurements indicated a transmission improvement to 66-70% at 1216 Å. This would indicate that the particular LiF boule used determines the transmission of windows cut from it.

1.4 Phosphor Output

1.4.1 Resolution

The resolution requirement for this tube dictated the use of the highest resolution P-11 phosphor available. Experience gained with the use of Reidel-de Haen phosphor indicated capability of 100-120 lp/mm at some sacrifice in efficiency because of the smaller "grain" size. Measurement performed on a typical plate used on the uv converter tube indicated 112 lp/mm.

1.4.2 Phosphor

A P-11 phosphor is used in the uv image converter. This phosphor is composed of ZnS:Ag and has a nominal efficiency of 10%; however, the use of the Reidel-de Haen material to achieve high resolution results in a lower efficiency because of the finer grain size. As shown in Figure 2, the spectral response is peaked at 4600 Å.

2. TUBE PROCESSING

The uv converter tubes are processed on a vacuum manifold pumped by both a Vac-Ion and Hg diffusion pumps. The silver chloride window seal limits bakeout temperature to 300°C which is performed overnight for a total of 15 hours. Photocathode processing is performed at approximately 1×10^{-9} Torr. The tube is operated with voltage after the nickel substrate deposition and after final photocathode processing. Tube aging is performed progressively from 10 kv to 30 kv for a 30-minute period. No detectable gas evolution is noted during tube aging and normally no spurious background or flashing is seen. The on-system aging permits evaluation of image linearity.

3. TUBE TEST

3.1 Spectral Response

During the initial development stages of this project, the CsI cathodes were processed for maximum response at 2537-3000 Å to facilitate testing. The spectral response curves of all three tubes measured are shown in Figure 3-a,-b, -c. The longer wavelength response can be controlled during processing, and it was determined that extreme solar blindness could be achieved by keeping the nickel substrate as thin as possible yet continuous to the extreme window edge for electrical contact. The tube is operated after nickel deposition with uv illumination to determine that complete coverage of the photocathode surface has been achieved. Processing of the final tubes (D-930 and D-931) indicate the feasibility of meeting the design goal that 3000 Å response be down by a factor of 10^4 or better from the 1216 Å figure.

3.2 Resolution

Operation of the first processed tube indicated that resolution measurements would be difficult because of the lower sensitivity at the uv wavelengths suitable for non-vacuum operation.

The photocathode window thickness of 3.8 mm precludes the possibility of using the test pattern against the window with collimated uv radiation because at a distance suitable to eliminate image spread the uv is too weak to permit visual observation.

Various combinations of uv sources, quartz-sapphire lens, and parabolic collimators were tried to increase the uv intensity at 1849 Å - 2537 Å without success. It was then decided to process a tube with a Rb_2Te photocathode to obtain sufficient sensitivity at 2537 Å air path to permit resolution measurements. This tube, designated D-933, made possible resolution measurements using the equipment as illustrated in Figure 4. Resolution as a function of resolution pattern position on the cathode was measured and is illustrated in Figure 5. These measurements were performed by reducing the aperture of a 1/2" diameter quartz plano-convex lens to 1/16". Visually element 4 of group 5 was resolved ($2 \times 45.6 = 91$ l_p/mm). The image quality without the aperture was degraded to the extent that proper resolution could not be obtained because of the poor optical image. A 2:1 image minification was realized so that the bimetal resolution test pattern was not limiting. A reproduction of the test pattern and description is included in the appendices (Figures I through IV). Microphotographs were taken by means of a lensless shutter attachment to a Polaroid camera using Polaroid type 510 film (ASA 10,000).

These photographs, because of the low light level involved, do not reproduce the resolution visually seen through the microscope. Typical photographs are shown in Figure 6.

3.3 Linearity

The equipment used for resolution measurement was also used in linearity measurements. The resolution test pattern was replaced by a screen pattern having a "cross" pattern at the center. The microscope is equipped with a reticule which permits centering of the cross pattern image. The tube was moved with respect to the fixed light spot image-microscope combination so that image rotation and non-linearity could be measured on a point-by-point basis. Since the screen pattern dimensions are known, displacement of the image in rotation, magnification, or non-linearity can be measured. A micro-photograph of the test pattern is illustrated in Figure 6 and in photographs of operating tubes shown in Figure 7.

Linearity data for tubes D-930 and D-931 operated in the permanent magnet is shown in Figures 8 through 11.

3.4 Gain

Gain has been measured two ways: (1) by a multichannel analyzer readout of single electron events from a photomultiplier tube coupled to the phosphor output plate and (2) by ratio of photocurrents of a photomultiplier coupled to the image tube. The accuracy of Method 1 is in question because of poor channel resolution and the decay time of the P-11 phosphor involved. The results obtained in Method 2 are outlined in detail.

Radiant gain, Gr, of the uv image converter tube was calculated from photocurrent measurements made on a coupled photomultiplier-uv image converter tube combination. The photomultiplier tube (D-716) was an EMR Model 541E-05M having a trialkali photocathode with a response peak of .084 A/W at 4100 Å. (Response curve included in Appendix VI). The uv image converter tube was exposed to 2537 Å incident radiation from a pen-ray lamp. The relationship of Gr, Gp (photon gain) and G_e (electron gain) is outlined below:

$$G_r = \frac{\text{output in watts}}{\text{input in watts}} \quad \text{at a given } \lambda \text{ in Angstrom units}$$

$$= \sigma_k V_{eff} \mathcal{E}$$

where σ_k is the uv cathode output in A/W at 1216 Å

V_{eff} is the uv image tube effective acceleration voltage

$\mathcal{E}$ is the phosphor efficiency in W/W.

$$G_p = \frac{\text{photons out}}{\text{photons in}} \quad \text{at a given } \lambda \text{ in Angstrom units}$$

$$= \text{Q.E. } V_{eff}\, \mathcal{E} = G_r \frac{\lambda \text{ out}}{\lambda \text{ in}} = \frac{4500 \text{ Å}}{1216 \text{ Å}}$$

$$G_e = \frac{\text{electrons from uv image converter tube}}{\text{electrons from photomultiplier cathode}}$$

$$= V_{eff}\, t\, \mathcal{E}\, k\, \sigma_2 \int P(\lambda) S(\lambda) d\lambda$$

$$= V_{eff}\, t\, \mathcal{E}\, \sigma_2 \;\; 0.850$$

where t = the coupling factor (uv tube to photomultiplier) was measured as being 0.6

$\mathcal{E}$ = phosphor efficiency in W/W

M_S = spectral matching factor computed from spectral curves of P-11 phosphor and photomultiplier tube (D-716) = 0.850

σ_2 = photomultiplier tube cathode response at 4100 Å = .084 A/W

$$\therefore \mathcal{E} = \frac{G_e}{V \times .043}$$

Values of G_e, G_r and G_p for the uv image converter tubes at various operating voltages are tabulated in Figure 12.

4. PACKAGING

4.1 Potting

One of the design goals was to maintain minimum length and diameter consistant with the primary objectives of resolution and linearity. The tube dimensions achieved permit an overall package including photomultiplier magnet of 4" nominal diameter and 4-1/2" length. Sufficient space exists between the kovar ring O.D. to bring both leads out the phosphor end of the tube. The lead insulation has been tested at 50 kv and by use of "flying leads" voltage breakdown and corona problems are eliminated in the vicinity of the tube.

A fiberglass housing with end caps is used to contain the silastic potting material and sufficient spacing is available around the rings so that adequate voltage insulation is provided between the rings and permanent magnet to permit 50 kv operation.

4.2 Magnet

Initial testing was performed using a solenoid type magnet permitting continuously variable magnet field strengths to 450 gauss. With an overall tube length of 3.5" and recessed input and output windows, magnet edge effects are minimized with the 6" long solenoid. Also, since the image size is 1" diameter, variations in the paraxial field of the 3" magnet are not severe.

In making the transition to the permanent magnet there are dimensional limitations because of magnet availability without resorting to special order magnets. The most promising magnet appeared to be a ring configuration consisting of two 2" long cemented rings having an O.D. of 4" and an I.D. of 3". Two such magnets were ordered at a paraxial field of 175 gauss. Field strength test of these magnets using a precision gaussmeter indicated a 550 gauss field in the center which dropped rapidly to 30-50 gauss at the edge. Poor linearity was obtained during operation of image tubes in these magnets. One magnet was separated by heating the epoxy cement. Various lengths of cold rolled steel rings were inserted between the two halves and improved operation was attained with a 1/4" thick section. The measured field strength was still too high at 250 gauss for 1st node operation and 2nd node operation was obtained on tubes operated in the permanent magnet configuration. A plot of magnet field strength is shown in Figure 13.

CONCLUSION

On the basis of test results obtained on completed tubes, the design objectives were essentially met. The paraxial resolution requirement of 50 lp/mm was exceeded but at the expense of some reduction in gain which is a result of the use of a high resolution phosphor. This is an area where trade-offs between resolution and gain can be varied to achieve the desired objectives.

A quantum efficiency of 10% was realized at 1216 Å with a 10^4 reduction in response at wavelengths of 3000Å and longer using a CsI photocathode. Completed tubes were free of spurious background and operation to 30 kv is possible with the proper magnet.

Overall package dimensions are well within the design objective of a maximum 6" diameter and 6" length.

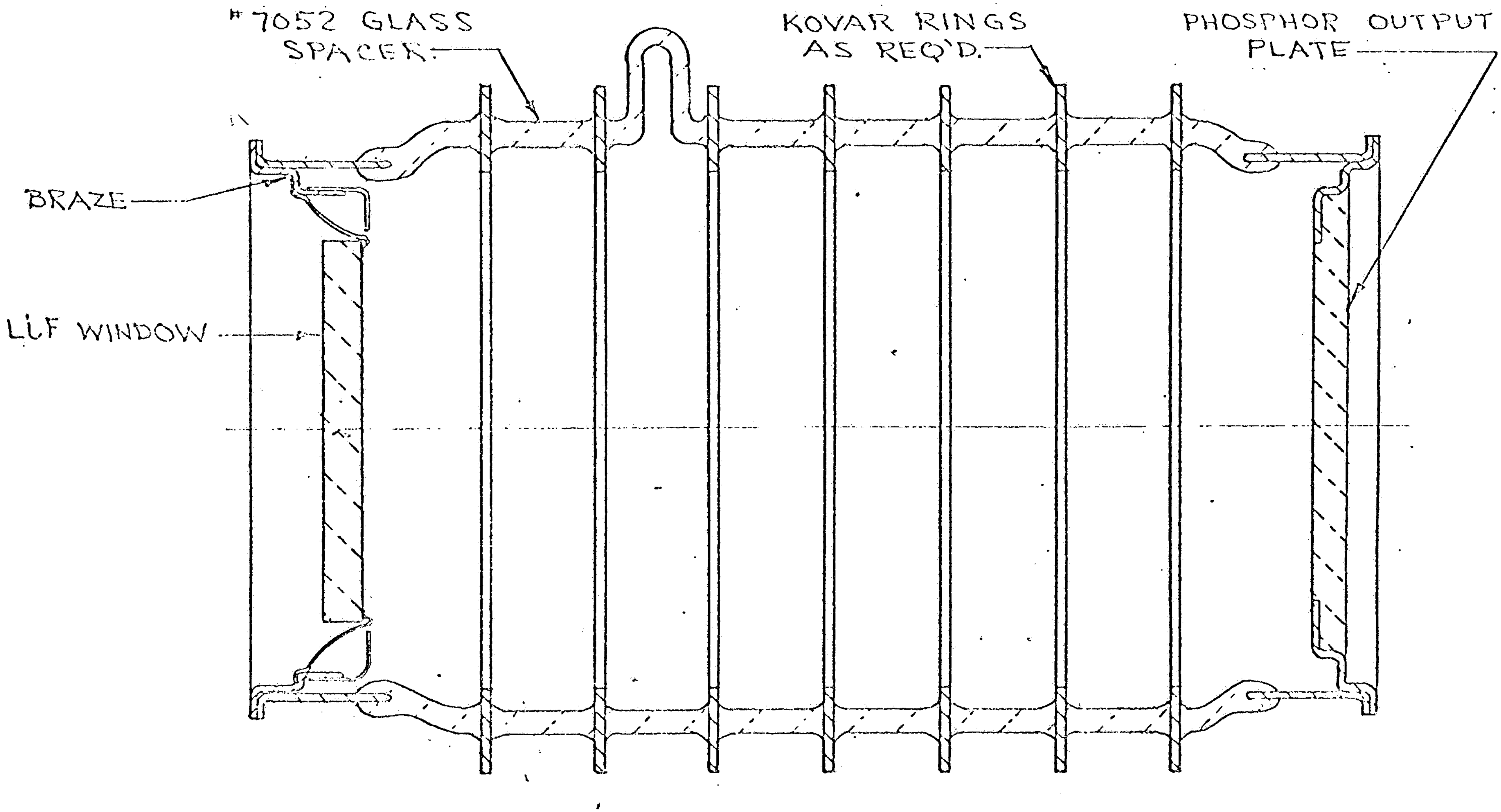

TUBE DRAWING
2 X SIZE

FIGURE 1

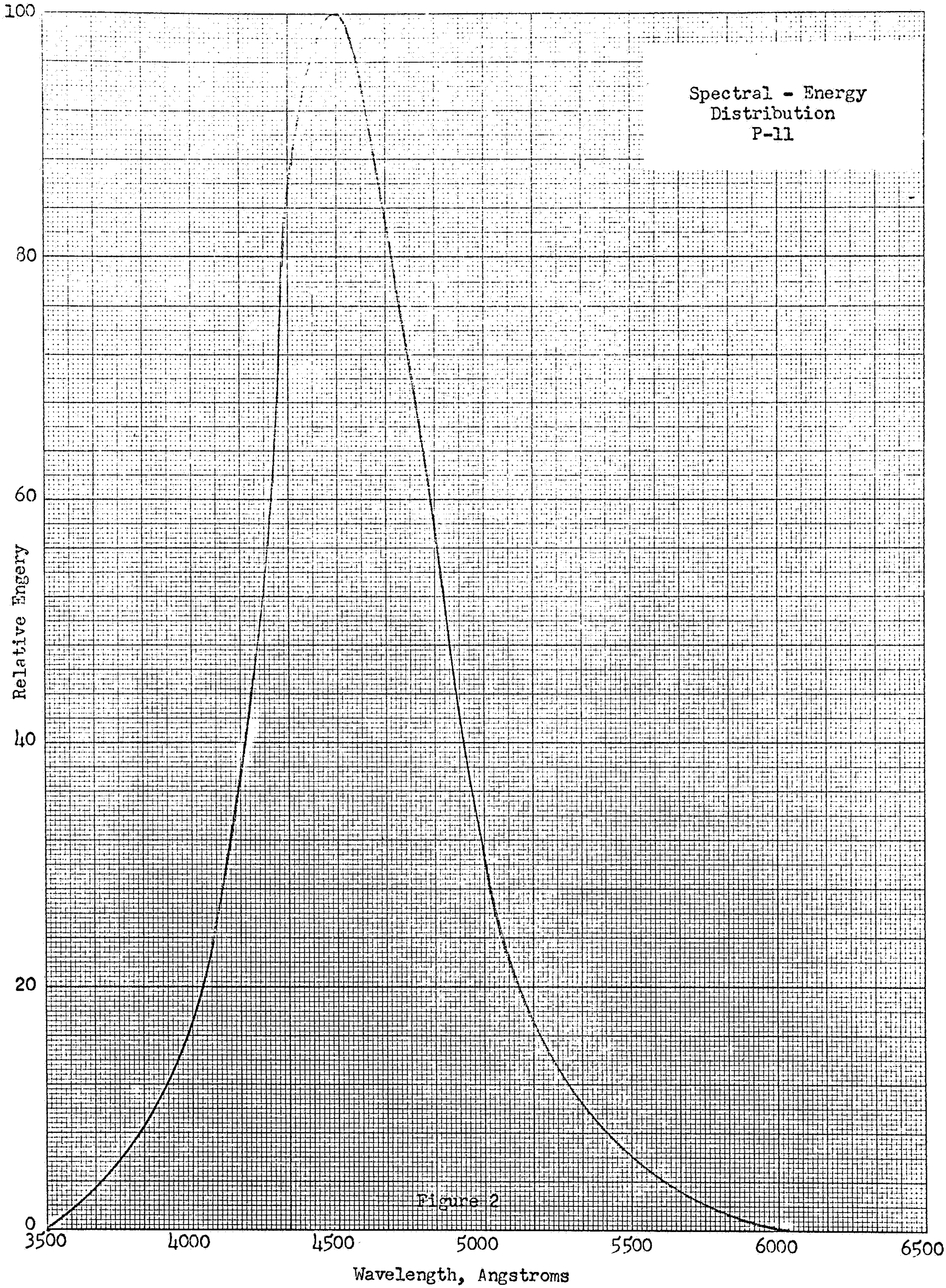
Spectral - Energy
Distribution
P-11
Relative Engery
100
80
60
40
20
0
3500
4000
4500
5000
5500
6000
6500
Wavelength, Angstroms

Figure 2

PHOTOMULTIPLIER SPECTRAL RESPONSE

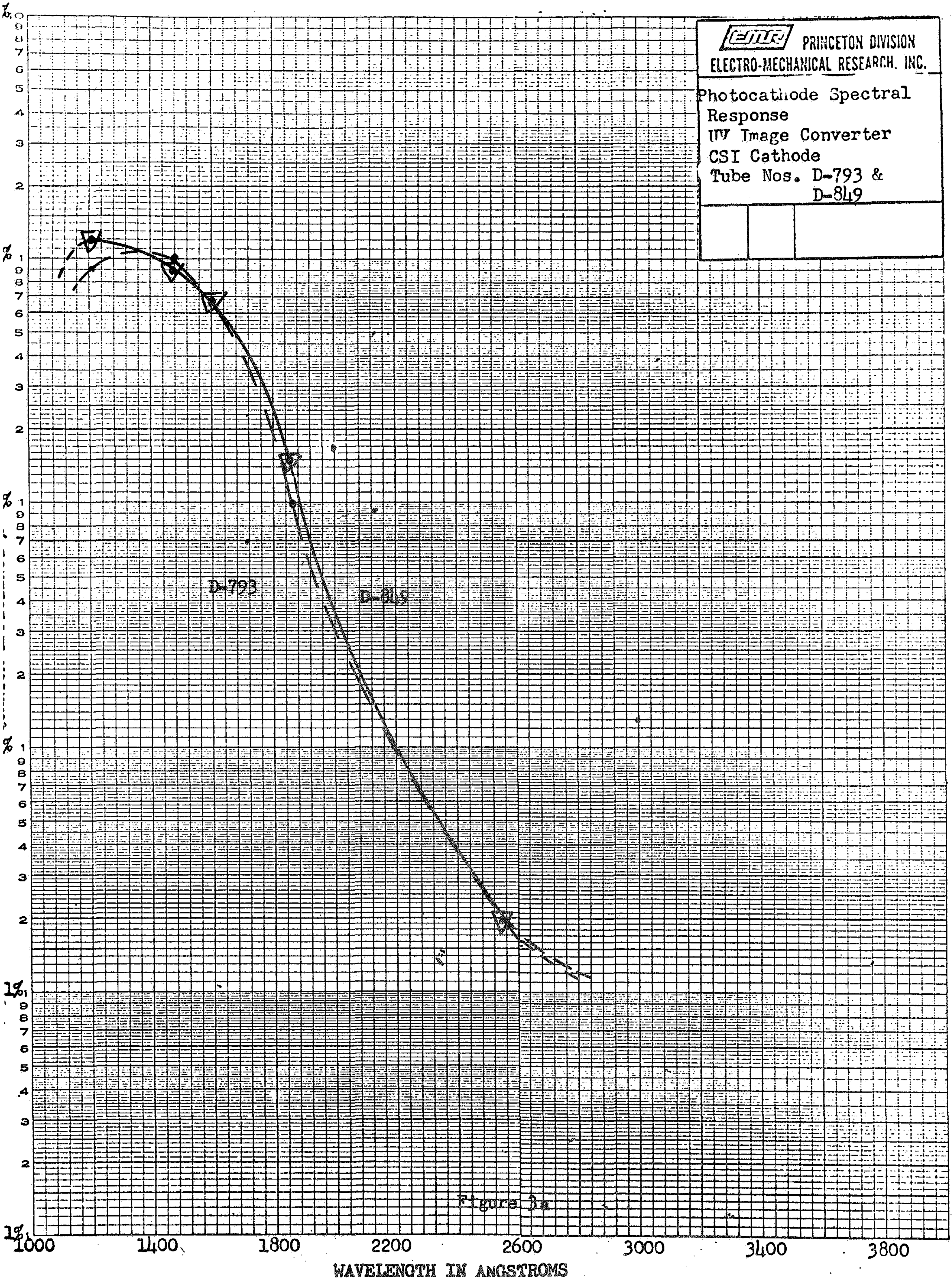

Figure 3a

PHOTOMULTIPLIER SPECTRAL RESPONSE

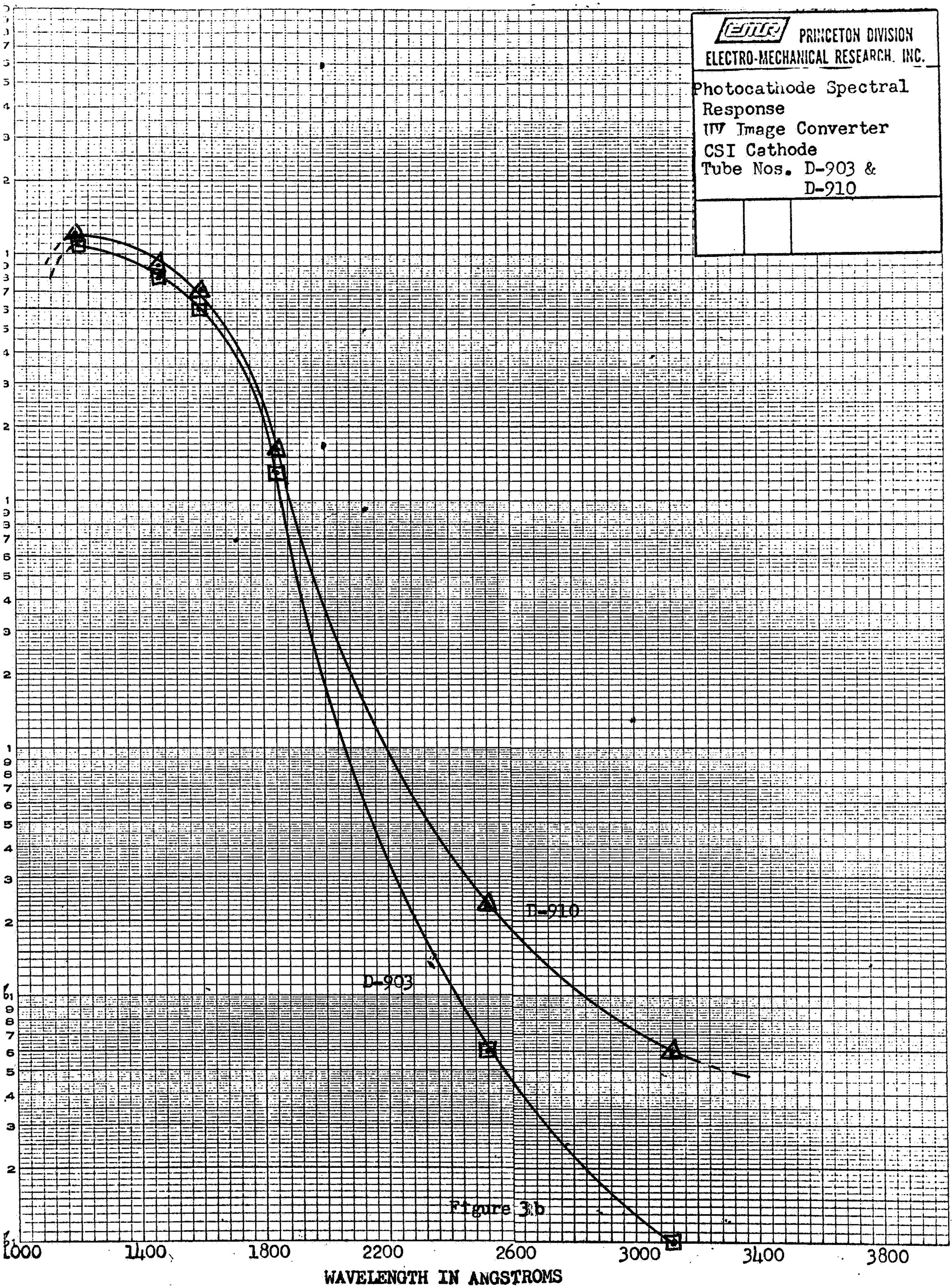

Figure 3b

PHOTOMULTIPLIER SPECTRAL RESPONSE

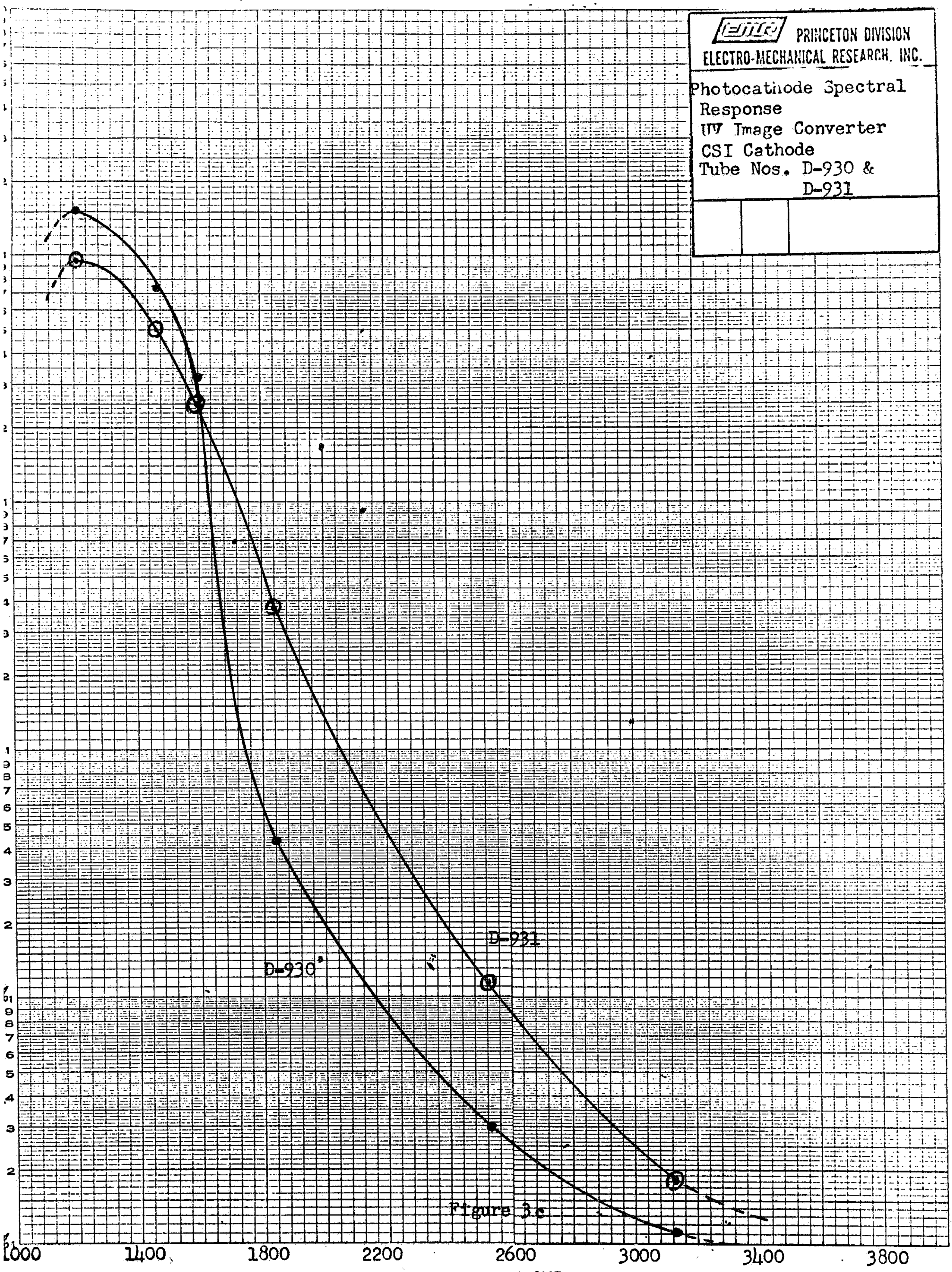

Figure 3c

WAVELENGTH IN ANGSTROMS

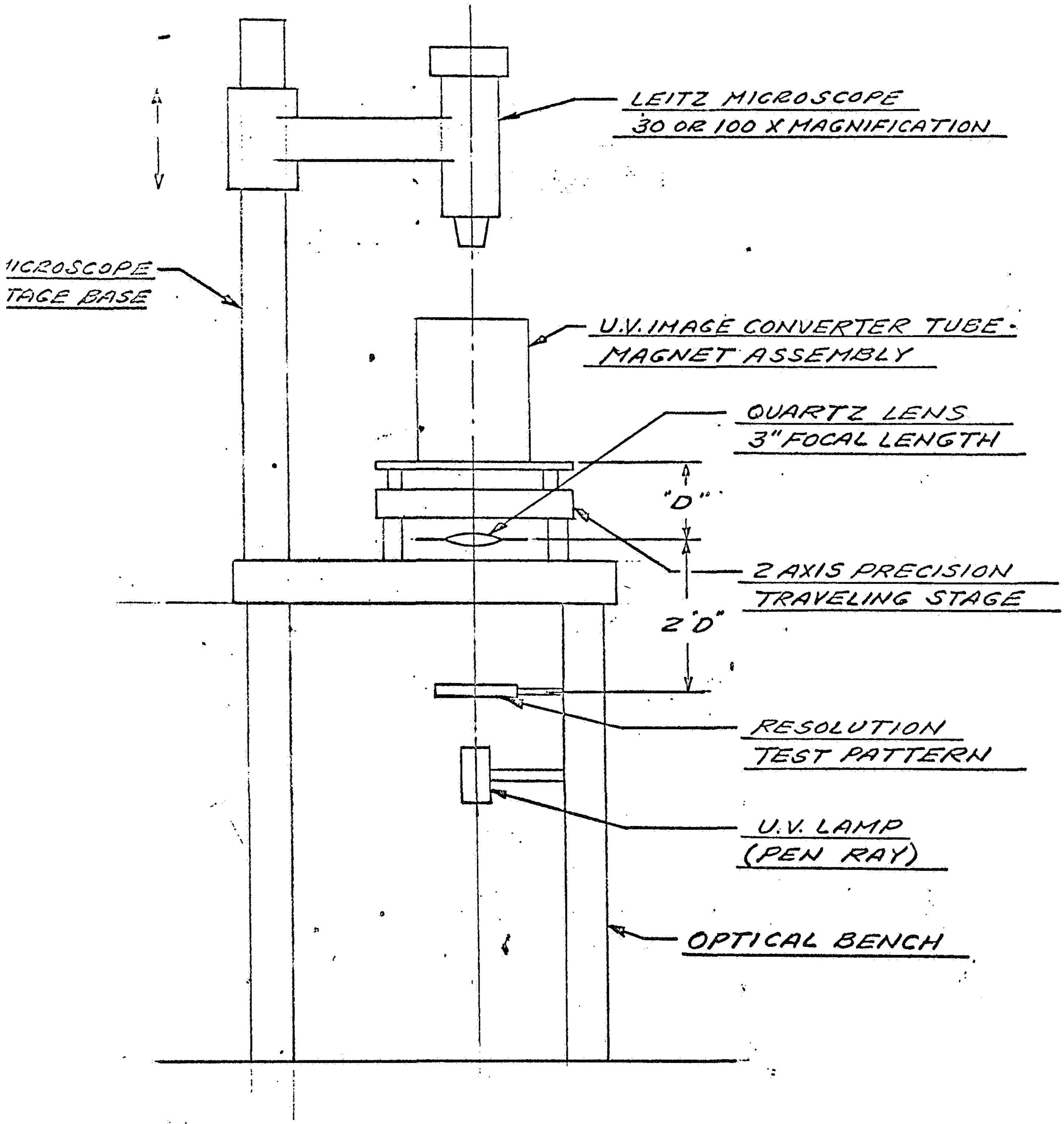

RESOLUTION-LINEARITY
TEST FIXTURE

Figure 4

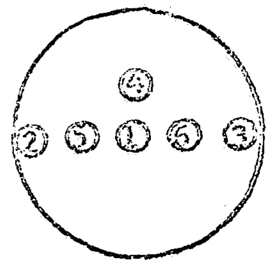

Position	Location
1	Center
2	Left edge (1/2" from center)
3	Right edge (1/2" from center)
4	1/4" above center
5	1/4" left of center
6	1/4" right of center

Tube Voltage (kv)	Focus Node	Focus Coil Current (ma)	Focus Coil Voltage (V)	Resolution lp/mm — Position Being Viewed 1	2	3	4	5	6
10	N_1	97	200	81	64	64	72	72	72
10	N_2	189	400	81	72	72	72	72	72
10	N_3	280	600	81	72	72	72	72	72
15	N_1	123	250	91	72	72	81	81	81
15	N_2	240	500	91	72	72	81	81	81
20	N_1	143	300	91	72	72	81	81	81
20	N_2	275	550	91	72	72	81	81	81
25	N_1	157	330	81	72	91	81	81	81
30	N_1	175	370	81	81	81	81	81	81
8	N_3	Permanent magnet operation		71	46	51	64	64	64
17	N_2	Permanent magnet operation		91	46	64	91	91	91

NOTE: Resolution measurements were made using a 2:1 minified optical image of the AF resolution test pattern as an input to the photocathode.

FIGURE 5

Summary of Resolution Measurements on D-933 Rb_2Te

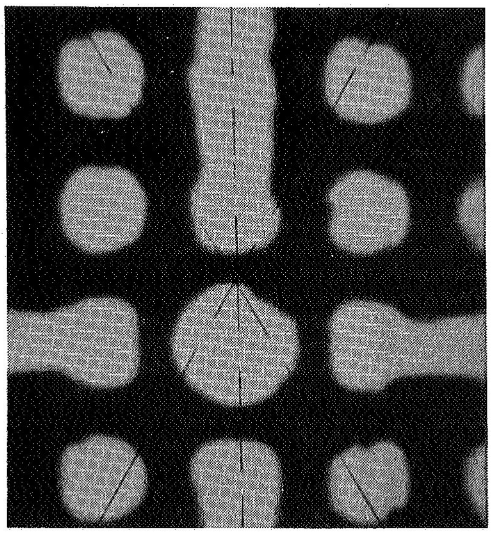

Fig. 6 (a)
D-930 P.M. at 15 KV
Linearity Test Pattern
Scale: 1cm = .215mm

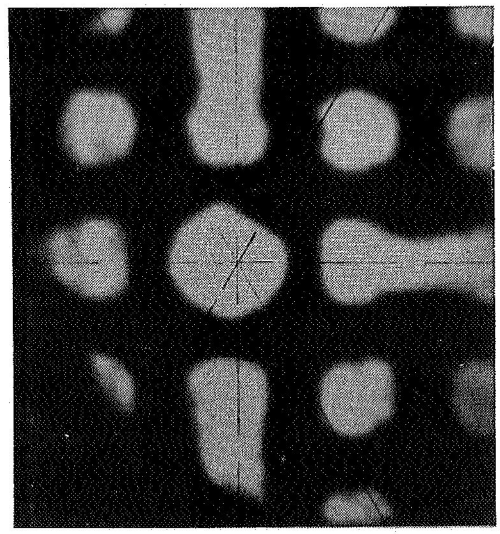

Fig. 6 (b)
D-931 P.M. at 16 KV
Linearity Test Pattern
Scale: 1cm = .215mm

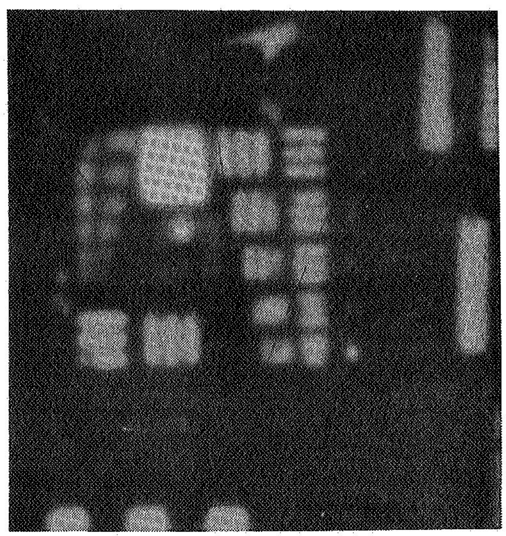

Fig. 6 (c)
D-933 P.M. at 20 KV
AF Resolution Test Pattern
Visual Resolution 91 LP/mm
ASA 10,000 Film at 5 sec. exp.
Camera Bellows Extended

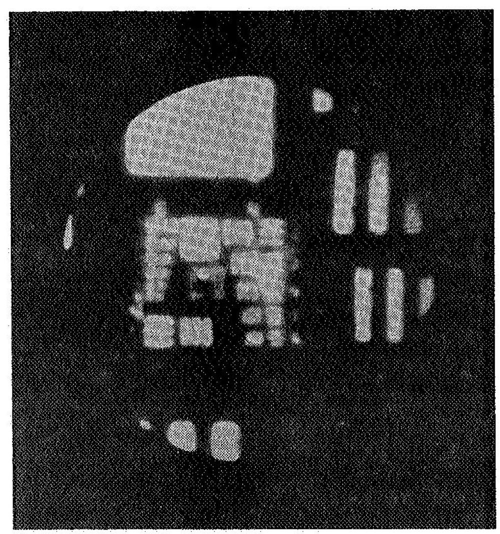

Fig. 6 (d)
D-933 P.M. at 20 KV
AF Resolution Test Pattern
Visual Resolution 91 LP/mm
ASA 10,000 Film at 2 sec. exp.
Camera Close to Microscope

FIGURE 6

MICROPHOTOGRAPHS OF OPERATING TUBES

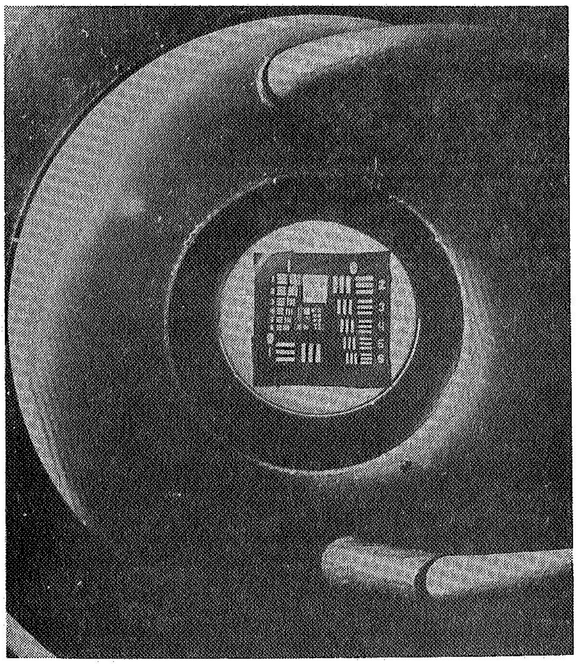

Fig. 7 (a)
Tube D-933 Rb_2Te
P.M. Operation at 20 KV
f 45 at 2.5 sec. exposure

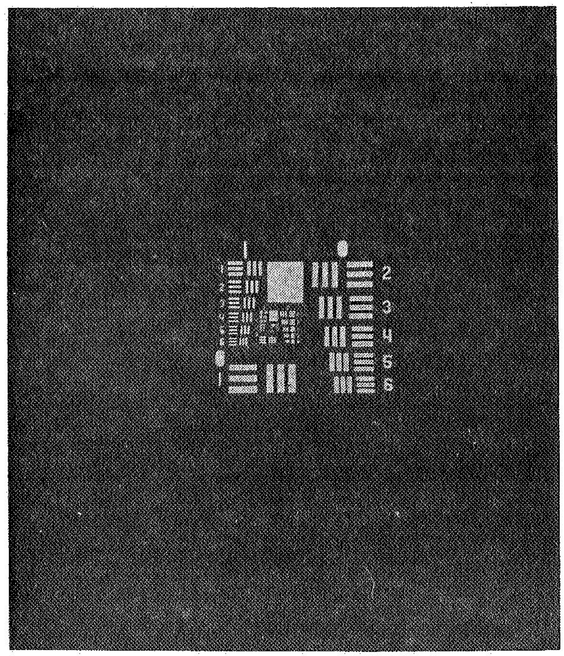

Fig. 7 (b)
D-933 P.M. Operation at 20 KV
Same as 7 (a) without side light
f 45 at 4 sec. exposure

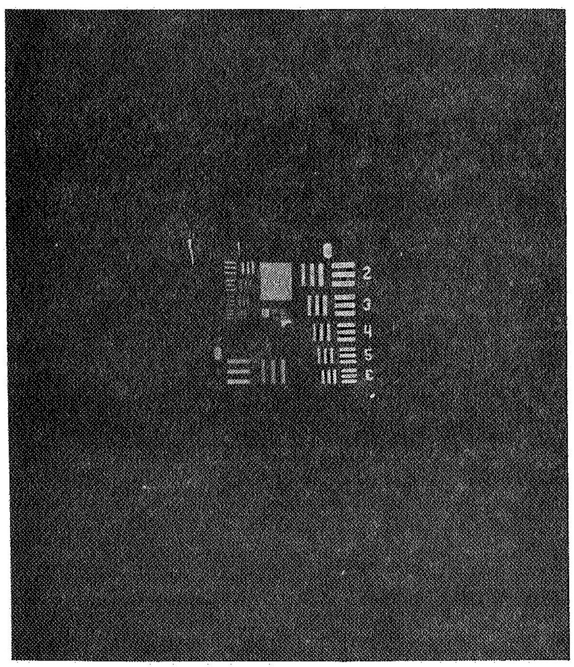

Fig. 7 (c)
D-930 CsI
P.M. Operation at 15 KV
f 16 at 30 sec. exposure

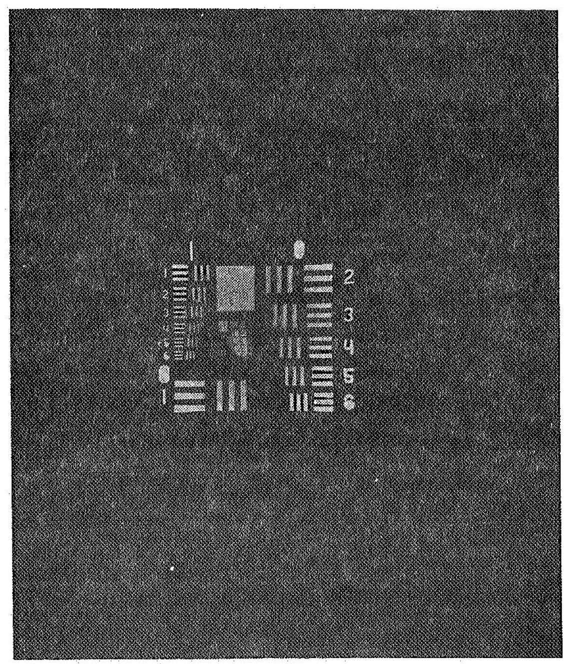

Fig. 7 (d)
D-931 CsI
P.M. Operation at 16 KV
f 16 at 30 sec.

FIGURE 7

PHOTOGRAPHS OF OPERATING TUBES
AF RESOLUTION TEST PATTERN AGAINST INPUT WINDOW
WITH 2537Å ILLUMINATION (32 LP/mm RESOLUTION)
POLAROID #510 FILM ASA 10,000

Horizontal Position Input Sig. (mm)	TUBE #D-930 P.M. Operation at 14.5 KV Output Sig. Displacement Hor.	TUBE #D-930 P.M. Operation at 14.5 KV Output Sig. Displacement Vert.	TUBE #D-931 P.M. Operation at 19.8 KV Output Sig. Displacement Hor.	TUBE #D-931 P.M. Operation at 19.8 KV Output Sig. Displacement Vert.
13	.48	2.36	1.72	.42
12	.54	2.04	1.50	.32
11	.54	1.83	1.32	.11
10	.48	1.61	1.29	0
9	.43	1.41	1.18	.107
8	.36	1.22	1.07	.14
7	.36	1.07	.97	.14
6	.32	.9	.90	.13
5	.27	.75	.75	.12
4	.26	.64	.57	.11
3	.21	.43	.45	.14
2	.11	.32	.32	.05
1	.05	.14	.11	.02
0	0	0	0	0
1	.05	.11	.17	0
2	.11	.26	.36	.05
3	.15	.43	.50	.07
4	.21	.54	.64	.11
5	.27	.75	.78	.11
6	.32	.97	.91	.11
7	.36	1.07	1.00	.11
8	.4	1.29	1.18	.07
9	.43	1.50	1.29	0
10	.45	1.77	1.50	.11
11	.45	1.93	1.75	.14
12	.43	2.26	1.93	.21
13	.43	2.47	2.15	.25

FIGURE 8

TABULATION OF MEASURED INPUT-OUTPUT

SIGNAL LINEARITY

TUBES D-930 & D-931 (PERM. MAGNET OPERATION)

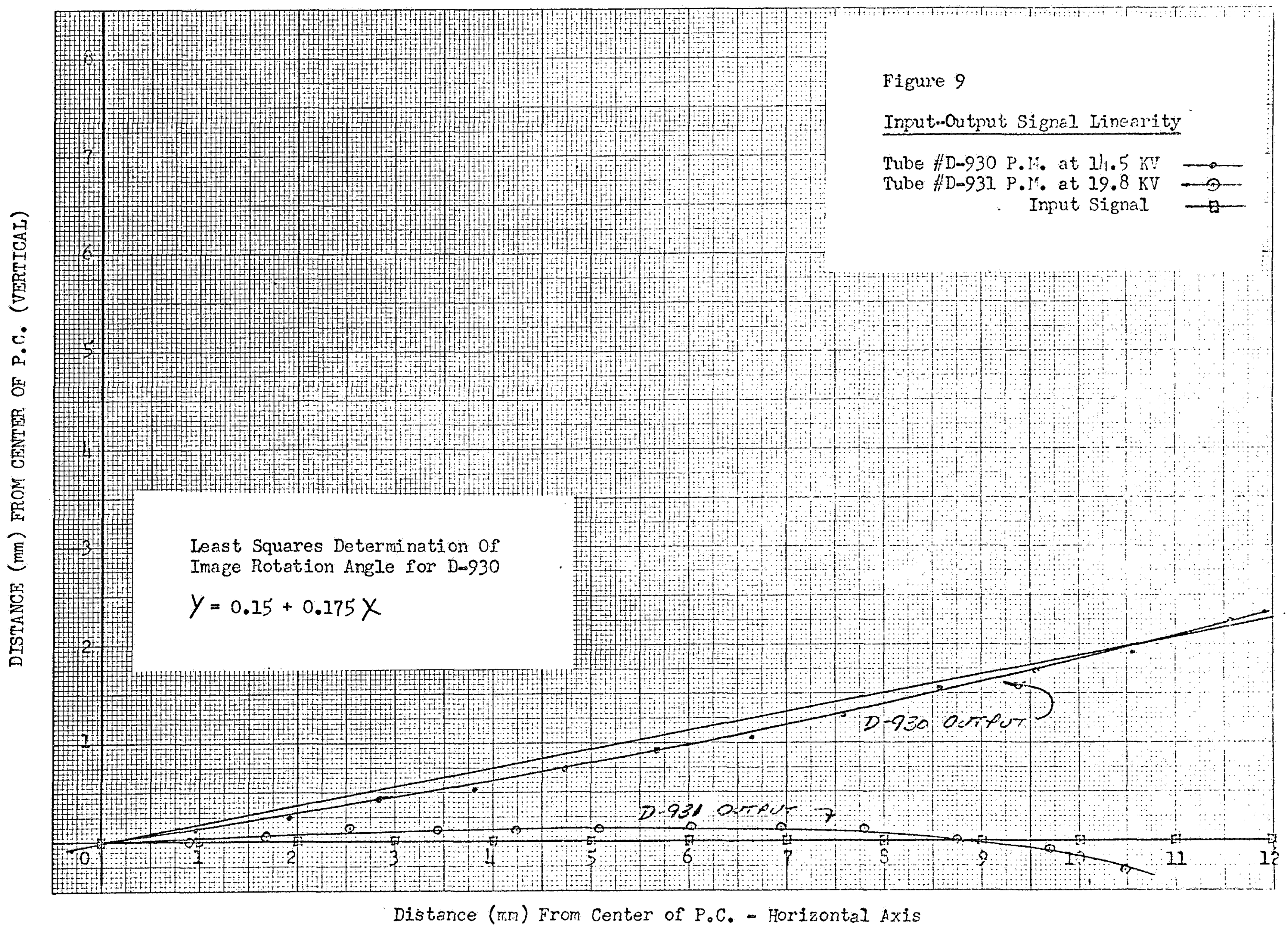
Figure 9
Input-Output Signal Linearity
Tube #D-930 P.M. at 14.5 KV
Tube #D-931 P.M. at 19.8 KV
Input Signal
Least Squares Determination Of
Image Rotation Angle for D-930
Y = 0.15 + 0.175 X
D-930 OUTPUT
D-931 OUTPUT
DISTANCE (mm) FROM CENTER OF P.C. (VERTICAL)
Distance (mm) From Center of P.C. - Horizontal Axis

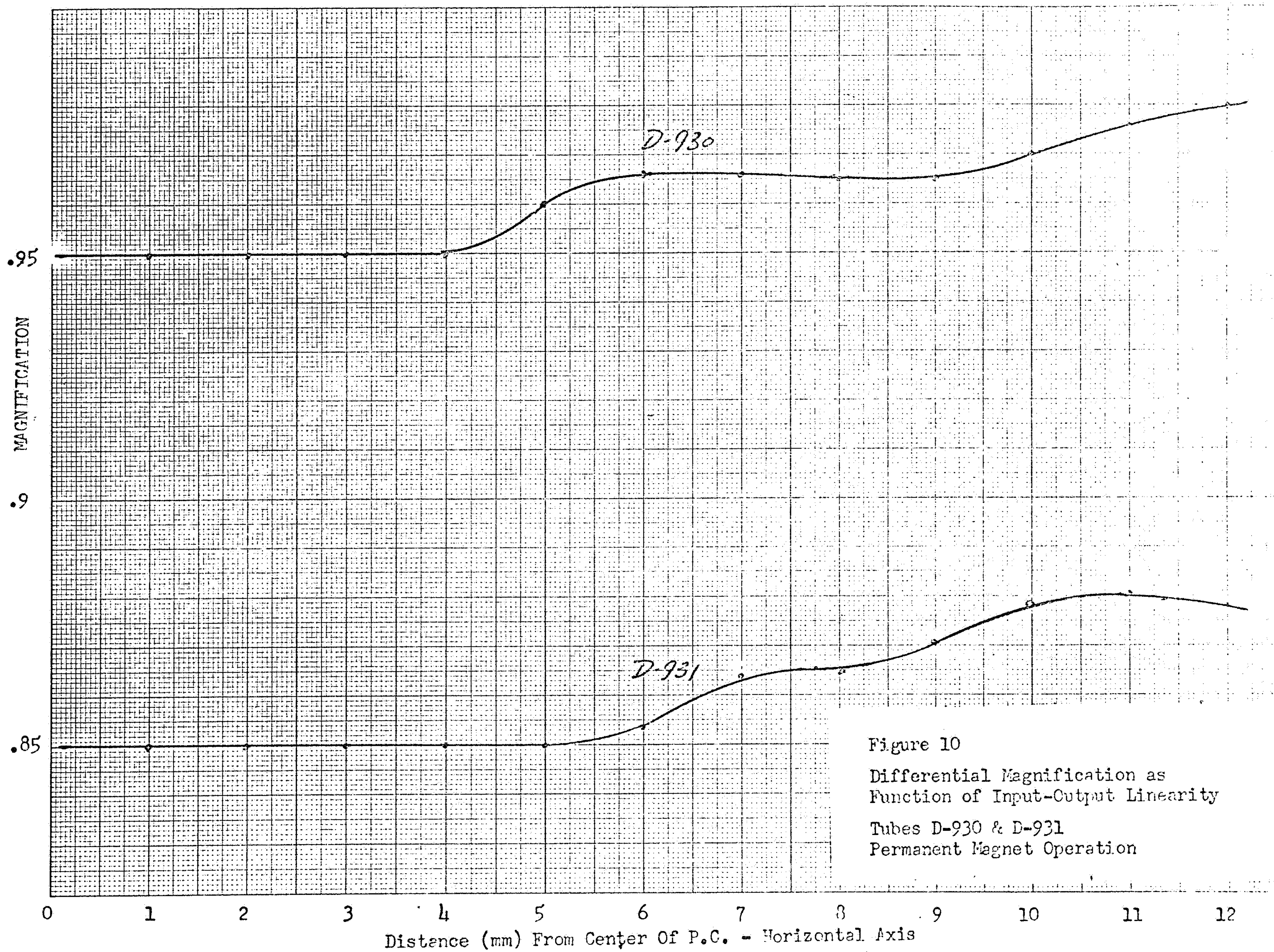

Figure 10

Differential Magnification as
Function of Input-Output Linearity

Tubes D-930 & D-931
Permanent Magnet Operation

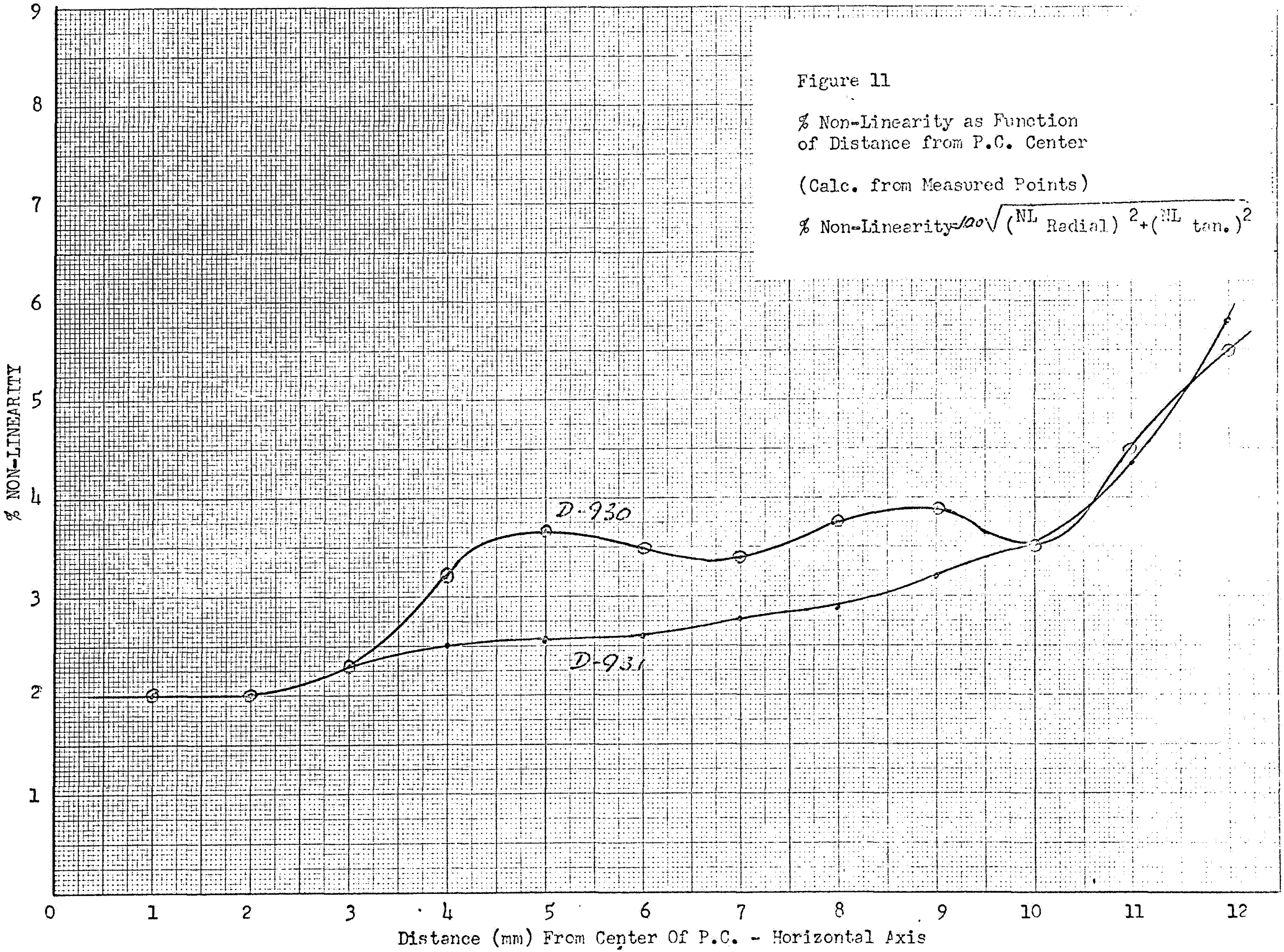

Figure 11

% Non-Linearity as Function of Distance from P.C. Center

(Calc. from Measured Points)

% Non-Linearity $= 100\sqrt{(NL\ \text{Radial})^2 + (NL\ \text{tan.})^2}$

Q.E.	Accelerating Voltage KV	Ge (MEAS)	E (CALC)	Gr (CALC) $\lambda = 1216 Å$	Gp (CALC) $\lambda = 1216 Å$
UV IMAGE TUBE D-930 CsI					
1216Å = 0.15	15	32.7	.051	11.4	42.5
2537Å =	20	43	.050	15	56
.00003	25	45	.042	15.7	58.4
UV IMAGE TUBE D-931 CsI					
1216Å = .095	15	20.8	.032	4.5	16.9
2537Å =	20	28	.032	6.1	22.7
.000015	25	32.3	.030	7.1	26.5
UV IMAGE TUBE D-933 Rb_2Te					
1216Å = .09	15	43	.068	10.2	38
2537Å =	20	53	.062	12.4	46.2
0.1	25	58	.054	13.5	50.3
UV IMAGE TUBE D-910 CsI					
1216Å = 0.12	15	48.2	.075	13.5	50.3
2537Å =	20	56	.065	15.6	58
.00023	25	55	.051	15.3	57

FIGURE 12

TABULATION OF GAIN FOR UV IMAGE CONVERTER TUBES

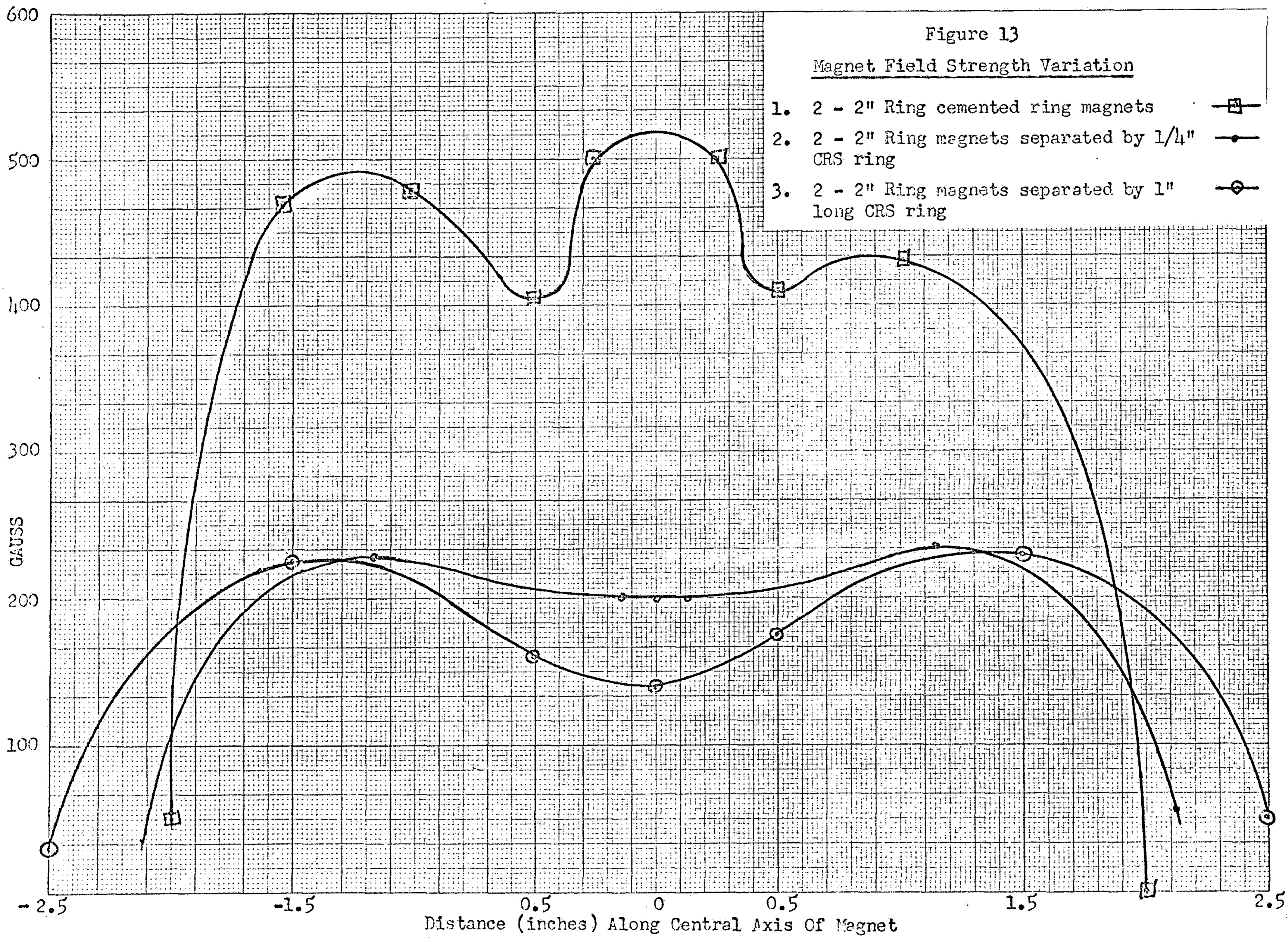
Figure 13
Magnet Field Strength Variation
1. 2 - 2" Ring cemented ring magnets
2. 2 - 2" Ring magnets separated by 1/4" CRS ring
3. 2 - 2" Ring magnets separated by 1" long CRS ring
600
500
400
300
GAUSS
200
100
-2.5
-1.5
0.5
0
0.5
1.5
2.5
Distance (inches) Along Central Axis Of Magnet

APPENDICES

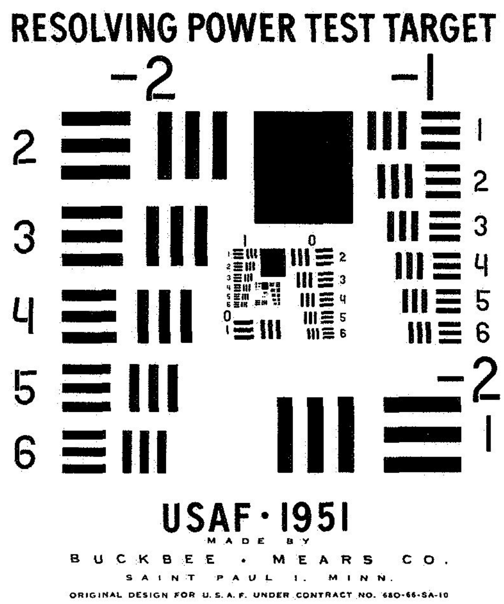
RESOLVING POWER TEST TARGET
USAF · 1951
MADE BY
BUCKBEE · MEARS CO.
SAINT PAUL 1, MINN.
ORIGINAL DESIGN FOR U. S. A. F. UNDER CONTRACT NO. 680-66-SA-10

APPENDIX I

U. S. A. F.

RESOLUTION CHART DATA

PREPARED BY

BUCKBEE MEARS COMPANY

ST. PAUL 1, MINN.

NOMENCLATURE AND SPECIFICATIONS

Interval—a line or a space.

Unit—a line and the adjacent space.

Pattern—three lines and two included spaces.

Element—an arrangement of two patterns set at right angles to each other and separated by one unit width.

The proportionality of the line and element dimensions is given by the ratio of the unit widths of two subsequent elements. This ratio shall be the sixth root of two. At the head of every group shall be a group number indicating the number of li/mm of the largest pattern within the group in terms of powers of two. For example, a group number K-3 shall indicate eight li/mm for the largest pattern of this group. The group numbers shall be whole numbers, for example—1, 0, 1 etc. Within a group, every element shall be designated by an element number n=1 (number 1 belonging to the largest element) through number 6 (number 6 belonging to the smallest element). The resolving power R represented by the element n of group K of the target can then be calculated from the equation.

$$R = 2^{\frac{K \text{ plus } n-1}{6}}$$

Thus element 1 of group —2 has 0.25 li/mm, element 1 of group —1 has 0.5 li/mm, and element 1 of group 0 has 1 li/mm.

The range of the target shall include ten target groups from 0.25 to 227.5 li/mm or from group —2 to group 7.

GROUP —2

(1) .25 li. m/m
- Interval = .07874
- Unit = .15748
- Element .94488 × .3937

(2) .280625 li. m/m
- Interval = .07014699
- Unit = .14029398
- Element .84176388 × .35073495

(3) .317475 li. m/m
- Interval = .06200488225
- Unit = .1240097645
- Element .744058587 × .31002441125

(4) .356175 li. m/m
- Interval = .0552677756
- Unit = .1105355513
- Element .6632133078 × .27633887825

(5) .3994 li. m/m
- Interval = .0492864296
- Unit = .0985728592
- Element .5914371552 × .246432148

(6) .44545 li. m/m
- Interval = .04419126725
- Unit = .0883825345
- Element .5302952124 × .2209563385

GROUP —1

(1) .50 li. m/m
- Interval = .03937
- Unit = .07874
- Element .47244 × .19685

(2) .56125 li. m/m
- Interval = .03507349665
- Unit = .0701469933
- Element .4208819598 × .17536748325

(3) .63495 li. m/m
- Interval = .0310024411
- Unit = .0620048822
- Element .3720292932 × .1550122055

(4) .71235 li. m/m
- Interval = .0276338878
- Unit = .0552677756
- Element .3316066536 × .138169439

(5) .7988 li. m/m
- Interval = .0246432148
- Unit = .0492864296
- Element .2957185776 × .123216074

(6) .8909 li. m/m
- Interval = .0220956336
- Unit = .0441912672
- Element .2651476032 × .110478168

GROUP+0

(1)	1 li. m/m	Interval = .019685	Unit = .03937	Element .23622 × .098425
(2)	1.1225 li. m/m	Interval = .01753674832	Unit = .03507349665	Element .2104409799 × .087683741625
(3)	1.2599 li. m/m	Interval = .01550122056	Unit = .03100244113	Element .18601464678 × .077506102825
(4)	1.4142 li. m/m	Interval = .01381694391	Unit = .02763388783	Element .16580332698 × .069084719575
(5)	1.5874 li. m/m	Interval = .01232160741	Unit = .02464321482	Element .14785928892 × .06160803705
(6)	1.7818 li. m/m	Interval = .01104781681	Unit = .02209563362	Element .13257380172 × .05523908405

GROUP+1

(1)	2 li. m/m	Interval = .0098425	Unit = .019685	Element .11811 × .0492125
(2)	2.245 li. m/m	Interval = .00876837416	Unit = .01753674832	Element .10522048992 × .0438418708
(3)	2.5398 li. m/m	Interval = .00775061028	Unit = .01550122056	Element .0900732336 × .0387530514
(4)	2.8494 li. m/m	Interval = .00690847195	Unit = .01381694391	Element .08290166346 × .034542359775
(5)	3.1952 li. m/m	Interval = .0061608037	Unit = .01232160741	Element .07392964446 × .030804018525
(6)	3.5636 li. m/m	Interval = .0055239084	Unit = .01104781681	Element .06628690086 × .027619542025

GROUP+2

(1)	4 li. m/m	Interval = .00492125	Unit = .0098425	Element .059055 × .02460625
(2)	4.49 li. m/m	Interval = .00438418708	Unit = .00876837416	Element .05261024496 × .0219209354
(3)	5.0796 li. m/m	Interval = .00387530514	Unit = .00775061028	Element .04650366168 × .0193765257
(4)	5.6988 li. m/m	Interval = .003454235975	Unit = .00690847195	Element .0414508257 × .017271177375
(5)	6.3904 li. m/m	Interval = .00308040185	Unit = .0061608037	Element .0369648222 × .01540200925
(6)	7.1272 li. m/m	Interval = .0027619542	Unit = .0055239084	Element .0331434504 × .013809771

GROUP+3

(1)	8 li. m/m	Interval = .002460625	Unit = .00492125	Element .0295275 × .012303125
(2)	8.98 li. m/m	Interval = .002192093541	Unit = .00438418708	Element .02630512248 × .0109604677
(3)	10.1592 li. m/m	Interval = .001937652571	Unit = .003875305142	Element .023251830852 × .009688262855
(4)	11.3976 li. m/m	Interval = .001727117989	Unit = .003454235979	Element .020725415874 × .0086355899475
(5)	12.7808 li. m/m	Interval = .001540200926	Unit = .003080401852	Element .018482411112 × .00770100463
(6)	14.2544 li. m/m	Interval = .001380977101	Unit = .002761954203	Element .016571725218 × .0069048855075

GROUP + 4

(1) 16 li. m/m
Interval = .0012303125
Unit = .002460625
Element .01476375 × .0061515625

(2) 17.96 li. m/m
Interval = .00109604677
Unit = .002192093541
Element .013152561246 × .0054802338525

(3) 20.3184 li. m/m
Interval = .000968826285
Unit = .001937652571
Element .011625915426 × .0048441314275

(4) 22.7952 li. m/m
Interval = .000863558994
Unit = .001727117989
Element .010362707934 × .0043177949725

(5) 25.5616 li. m/m
Interval = .000770100463
Unit = .001540200926
Element .009241205556 × .003850502315

(6) 28.5088 li. m/m
Interval = .000690488550
Unit = .001380977101
Element .008285820606 × .0034524252525

GROUP + 5

(1) 32 li. m/m
Interval = .00061515625
Unit = .0012303125
Element .007381875 × .00307578125

(2) 35.92 li. m/m
Interval = .000548023385
Unit = .00109604677
Element .00657628062 × .002740116925

(3) 40.6368 li. m/m
Interval = .0004844131425
Unit = .000968826285
Element .00581295771 × .0024220657125

(4) 45.5904 li. m/m
Interval = .000431779497
Unit = .000863558994
Element .0051813053964 × .0021588772485

(5) 51.1232 li. m/m
Interval = .0003850502315
Unit = .000770100463
Element .004620602778 × .0019252511575

(6) 57.0176 li. m/m
Interval = .000345244275
Unit = .00069048855
Element .0041429313 × .001726221375

GROUP + 6

(1) 64 li. m/m
Interval = .000307578125
Unit = .00061515625
Element .0036909375 × .001537890625

(2) 71.84 li. m/m
Interval = .0002740116925
Unit = .000548023385
Element .00328814031 × .0013700584625

(3) 81.2736 li. m/m
Interval = .000242206571
Unit = .000484413142
Element .002906478852 × .001211032855

(4) 91.1808 li. m/m
Interval = .0002158897485
Unit = .000431779497
Element .002590676982 × .0010794487425

(5) 102.2464 li. m/m
Interval = .0001925251157
Unit = .0003850502315
Element .002310301389 × .00096262557875

(6) 114.0352 li. m/m
Interval = .0001726221377
Unit = .0003452442754
Element .0020714656524 × .0008631106885

GROUP + 7

(1) 128 li. m/m
Interval = .0001537890625
Unit = .000307578125
Element .00184546875 × .0007689453125

(2) 143.68 li. m/m
Interval = .0001370058463
Unit = .0002740116926
Element .0016440701556 × .0006850292315

(3) 162.5472 li. m/m
Interval = .0001211032856
Unit = .0002422065713
Element .0014532394278 × .00060551642825

(4) 182.3616 li. m/m
Interval = .0001079448743
Unit = .0002158897487
Element .0012953384922 × .00053972437175

(5) 204.4928 li. m/m
Interval = .0000962625578
Unit = .0001925251157
Element .0011551506942 × .00048131278925

(6) 228.0704 li. m/m
Interval = .0000863110688
Unit = .0001726221377
Element .0010357328262 × .00043155534425

300 li. m/m

$\frac{(20)}{1}$

Interval = .000065616666
Unit = .00013123333
.00078739998 × .000328083325
.0157479996 × .0065616666

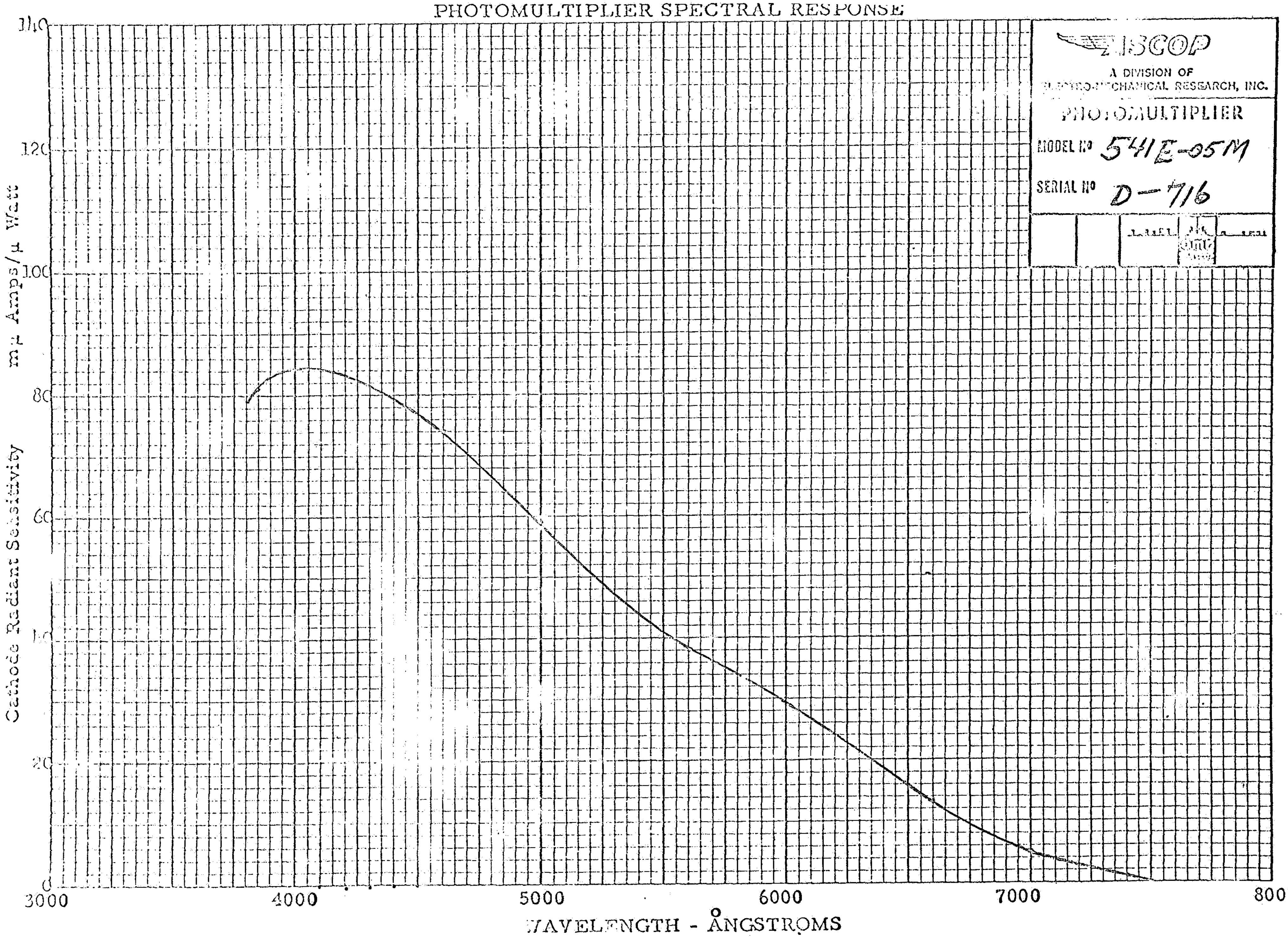

PHOTOMULTIPLIER SPECTRAL RESPONSE
A DIVISION OF
PHOTOMULTIPLIER
MODEL No 541E-05M
SERIAL No D-716
Cathode Radiant Sensitivity mμ Amps/μ Watt
140
120
100
80
60
40
20
0
3000
4000
5000
6000
7000
8000
WAVELENGTH - ÅNGSTROMS

APPENDIX V